Characterization of Mass and Swelling of Hydrogel Microstructures using MEMS Resonant Mass Sensor Arrays

*Larry J. Millet, Elise A. Corbin, Robert Free, Kidong Park, Hyunjoon Kong, William P. King, and Rashid Bashir**

The use of hydrogels for biomedical engineering, and for the development of biologically inspired cellular systems at the microscale, is advancing at a rapid pace. Microelectromechanical system (MEMS) resonant mass sensors enable the mass measurement of a range of materials. The integration of hydrogels onto MEMS resonant mass sensors is demonstrated, and these sensors are used to characterize the hydrogel mass and swelling characteristics. The mass values obtained from resonant frequency measurements of poly(ethylene glycol)diacrylate (PEGDA) microstructures match well with the values independently verified through volume measurements. The sensors are also used to measure the influence of fluids of similar and greater density on the mass measurements of microstructures. The data show a size-dependent increase in gel mass when fluid density is increased. Lastly, volume comparisons of bulk hydrogels with a range polymer concentration (5% to 100% (v/v)) show a non-linear swelling trend.

1. Introduction

Hydrogels are versatile materials used for biological and biomedical applications,[1] namely: drug delivery,[2] cell encapsulation,[3] cell migration,[4] tissue engineering,[5] and artificial cellular systems.[6] New methods are emerging for fabricating hydrogel-based cellular systems at the size-scale of cell populations and ultimately individual cells; thus, tools are needed to characterize material properties of microscale hydrogels.

Microelectromechanical system (MEMS) resonant mass sensors have been used for mass measurements of a range of substances, including viruses,[7] bacteria,[8] cells,[9–11] biochemicals,[11] and liquids and gases.[12] In addition to mass measurement of biological and chemical substances, materials characterization can also be performed through the use of MEMS mass sensors. For example, the physical characteristics of polymer coatings can be measured with cantilevers due to changes in electrostatic, steric, osmotic, or solvation forces that accompany physical changes in the polymer coatings.[13]

The most commonly used MEMS resonant mass sensors are cantilever structures, though the conventional cantilever sensors can exhibit >100% non-uniform mass sensitivity, since the location of the object to be measured relative to the free end determines the mass sensitivity.[14] We have recently developed an array of MEMS resonant mass sensors that solve the mass uniformity challenge inherent in cantilever sensors.[10,15] Our sensors consist of resonating platforms suspended by four angled beam springs, and achieve at least 96% uniformity of mass sensitivity across any point on the measurement platform. Operating in first resonance mode,

L. J. Millet,[+] R. Free, K. Park, R. Bashir
Department of Electrical and Computer Engineering
Micro and Nanotechnology Laboratory
University of Illinois Urbana-Champaign
Urbana, IL 61801, USA
E-mail: rbashir@illinois.edu

E. A. Corbin,[+] W. P. King
Department of Mechanical Engineering
Micro and Nanotechnology Laboratory
University of Illinois at Urbana-Champaign
Urbana, IL 61801, USA

H. J. Kong
Department of Chemical and Biomolecular Engineering
Micro and Nanotechnology Laboratory
University of Illinois at Urbana-Champaign
Urbana, IL 61801, USA

[+] L.J.M. and E.A.C. contributed equally to this work.

DOI: 10.1002/smll.201200470

the platform is driven with a Lorentz force and vibrates vertically in both air (~160 kHz) and liquid (~60 kHz). Our sensors have recently been used for direct measurements of cell mass and growth of adherent human cancer cells, showing that cell mass and growth can be measured for single cells.[10,15] Not only is the stabilization provided by the beam springs essential for restricting the resonance mode and enabling spatial uniformity in mass sensitivity, but the spring-platform structure is sufficiently robust to permit additional material fabrication protocols (such as surface functionalization, cell attachment, and photolithography) between measurements. These advantages provide measurement capabilities for studies on materials beyond what the traditional cantilever mass sensor could enable. This also allows for hydrogel structures to be studied using these sensors. It is difficult to attach prefabricated hydrogels individually to the surface of each suspended sensor, and thus the gels must be fabricated directly onto the devices.

The goal of this work is to demonstrate that material microstructures, specifically hydrogels, can be integrated with MEMS resonant mass sensors for materials characterization. Here, we use photolithography to fabricate poly(ethylene glycol) diacrylate (PEGDA) hydrogel microstructures onto the surface of the square resonant sensors. We estimate the mass of hydrogel structures using the sensors and verify the measurement using scanning electron microscopy (SEM). We also show that hydrogels can be fabricated to a range of sizes and can be measured under various fluidic conditions to provide insight on material characteristics of hydrogels under changing fluidic environments.

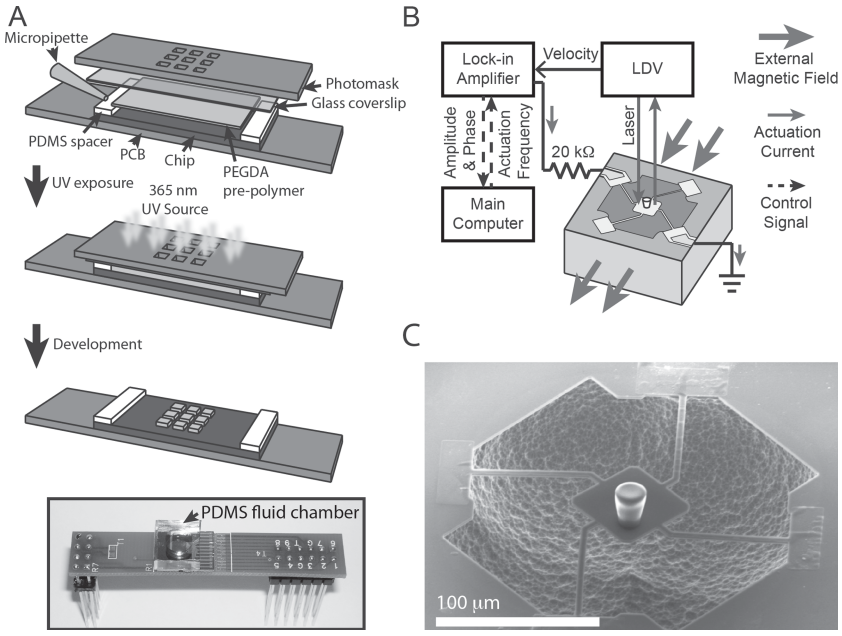

Figure 1. Experimental setup and measurement overview. A) Process overview of photolithographic fabrication of PEGDA-DMPA gel structures onto the MEMS resonant mass sensors (sensor platforms not shown). PEGDA-DMPA pre-polymer and PDMS spacers were sandwiched between the chip (with mass sensors) and coverslip. The chip-coverslip assembly was aligned, brought into contact with the photomask, exposed with 365 nm UV light, developed, and rinsed with DI water. Following lithography, the gels remain immersed in water in a PDMS chamber during measurements; a fully assembled chip is shown. For scale, the printed circuit board (PCB) measures 6.3 cm (length, *l*), 1.1 cm (width, *w*). B) Schematic representation of the measurement set up for measuring the resonant frequency of MEMS resonant mass sensors with laser Doppler vibrometery (LDV).[10] C) Scanning electron microscopy (SEM) image shows the MEMS mass sensor with a PEGDA-DMPA hydrogel structure fabricated through photolithography onto the suspended platform. For scale, the square platform measures 60 μm × 60 μm.

2. Materials and Methods

2.1. MEMS Resonant Mass Sensors

The fabrication of the MEMS resonant mass sensor array has been previously reported and is only summarized here.[10] The mass sensor array is formed from a silicon-on-insulator wafer with device layer (2.0 μm) and a buried oxide layer (0.3 μm). A silicon dioxide layer is used as an electrical insulation layer. Chrome and gold layers are deposited, patterned, and etched to form the springs and platforms. Electrical leads and bonding pads are formed with additional chrome and gold layers. Xenon difluoride (XeF_2) etching is used to form a "pit" beneath the platform and springs to release the sensor platform. The device is cleaned and a silicon dioxide layer is deposited for insulation; the final oxide is selectively removed from the bonding pad area for wire-bonding. After chip fabrication, the chip is attached to a custom printed circuit board and wire-bonded.

2.2. Mass Measurements

The mass of the hydrogel was obtained from the difference of the resonant frequencies of the empty sensor and the sensor with gel. The measurement of the resonant frequency was fully automated as shown in **Figure 1**. Briefly, Lorentz force is induced by flowing actuation current through the sensor in a static magnetic field for electromagnetic actuation and laser Doppler vibrometry (LDV; OFV 3001 vibrometer controller and OFV 512 fiber interferometer, Polytec Inc.) is used to measure the resulting velocity of the vibrating platform. The resonant frequency was estimated by comparing the phase of the sensor velocity and that of the actuation current. Since the spring constant of the sensor structure does not change, the mass of the patterned hydrogel can be solely determined from the resonant frequency, and a series of resonant frequency measurements enables monitoring the mass change.[10]

Precise extraction of the sample mass requires resonant frequencies to be measured for each sensor in three different

small 2012,
DOI: 10.1002/smll.201200470

NANO MICRO small

scenarios, a) empty sensors in air, b) empty sensors in fluid pre-lithography, and c) sensors with gels post-lithography. The resonant frequency of each sensor of the array is first measured in air to extract the spring constant, k, in the following equation: $m_{gel} = \frac{k}{4\pi^2}(f_{wet\_gel}^{-2} - f_{wet\_empty}^{-2})$. Then, the resonant frequency of each sensor is measured in fluid before and after hydrogel fabrication, which are f_{wet_empty} and f_{wet_gel}, respectively. The measured resonant frequency shift is determined and ultimately converted to the mass of the gel, m_{gel} on each of the individual sensors. To obtain the final mass of the microstructures without influences of frequency drift, mass readings of adjacent empty sensors are subtracted from the initial mass results.[10]

The mass of hydrated 100% PEGDA-(2,2′-dimethoxy-2-phenylaxetophenone) DMPA hydrogel microstructures in fluids of various densities was determined by: a) first measuring the gels in deionized (DI) water (0.99 g/cm^3) after reaching equilibrium, b) followed by a fluid rinse with, and a change to, the density matched solution (73% glucose, 1.13 g/cm^3) similar to the density of 100% PEGDA-DMPA (1.124 g/cm^3). c) The gels were then rinsed with and measured in the higher-density solution (80% glucose, 1.23 g/cm^3), d) followed by rinsing with, then incubation in, DI water prior (>24 h) to a second mass measurement in DI water. e) Lastly, the gels were dried and measured in air to permit the calculation of the mass swelling ratio (Q_m) for determining the Q-factor for comparison to bulk discs.

2.3. Surface Chemistry

Surface chemistry was performed in order to functionalize the sensor array with methacrylate groups so as to promote hydrogel microstructure adherence during photolithography. The arrays were cleaned with oxygen plasma (1 min) (Diener Electronic; Ebhausen, Germany). Immediately after cleaning, the sensors were then methacrylated by applying 3-acryloxypropyl trimethoxysilane (5–10 μL) (Gelest, Inc.; Morrisville, PA, USA) directly onto the sensor array and then heated (70 °C, 30–60 min) in a closed Petri dish. Samples were then gently rinsed with acetone and methanol, dried, and used for photolithography within a few days.

To form thin fluidic layers of hydrogel pre-polymer and facilitate the retention of standing isolated hydrogel structures, silanized coverslip fragments were placed on polydimethylsiloxane (PDMS) spacers. Silanized coverslip fragments (approx. 1 cm × 1 cm, #1 thickness) used in the lithography process were prepared by first cleaning the glass with oxygen plasma for 1 min followed by direct exposure to dimethyl(3,3,3, trifluoropropyl)chlorosilane (10–15 μL) at room temperature (22 to 24 °C) in a vacuum chamber (at least 1–2 h). Coverslips were rinsed with ethanol and dried with a nitrogen stream.

2.4. PEGDA-DMPA Hydrogel Solutions

The PEGDA-DMPA hydrogel solution comprises a poly(ethylene glycol)diacrylate (PEGDA; molecular weight, MW 575) and a photoinitiator, 2,2′-dimethoxy-2-phenylaxetophenone (DMPA). Stock solutions of 10–20 mg DMPA per mL PEGDA were prepared and allowed to mix (1–4 h) before use. In this study, hydrogels were microfabricated from undiluted stock PEGDA-DMPA solutions (100% PEGDA-DMPA). To ultimately calculate hydrogel mass from volume measurements, the density of hydrogel pre-polymer was calculated by measuring the mass of defined volumes of PEGDA-DMPA pre-polymer deposited onto weigh boats on an analytical balance. Lower percent gel formulations are 100% PEGDA-DMPA diluted with water. All PEGDA-DMPA pre-polymer preparations were performed under yellow lighting conditions; reagents are stored with protection from light.

2.5. Photolithography

Figure 1A shows an overview of the photolithography process for PEGDA hydrogel structures on the MEMS sensor array. Hydrogel microstructures were patterned from the PEGDA-DMPA pre-polymer solution described above. The solution acts as a negatively toned photoresist; regions exposed to UV light undergo a free radical polymerization reaction and become insoluble in the developer (DI water). To control the approximate structure thickness, PDMS thin-films were used as spacers (10–50 μm thick) to hold the glass coverslip above the sensor chip. The PEGDA-DMPA pre-polymer solution (3–5 μL) was applied directly to the chip with a pipette and gently covered by a silanized coverslip fragment. In this process, capillary action distributes the solution across the chip and any excess solution can be wicked away with a Kim wipe to ensure a tight coverslip fitting due to the surface tension of the pre-polymer. The photomask was aligned to the sensor array in the mask aligner, brought into hard contact with the coverslip, and exposed to 9.4 mW cm^{-2} of 365 nm UV radiation (1–3 min), a time predetermined by iterative exposures. Finally, the coverslip-chip-PCB assembly was removed from the aligner and developed by perfusing DI water through the fluid-filled gap between the coverslip and the chip surface, until the pre-polymer is removed or the cover slip detaches.

2.6. Volume Calculations of Microstructures

Volume calculations of hydrogel structures used dimensions obtained from SEM images. To estimate volumetric mass of hydrogel structures, the air-dried 100% PEDGA hydrogel structures were imaged with a scanning electron microscope (SEM) in the Beckman ITG microscopy suite (University of Illinois Urbana-Champaign). Side profile and top view images were acquired in high-vacuum mode with 1 kV accelerating voltage, spot size 2.1 nm, and 2000× magnification.

Dimensions for the area (A) of the hydrogel top, the gel height (h'), the top width (w_{top}), and the gel bottom width (w_{bottom}) were used to calculate the volume of a frustum for estimating structure volume, as shown in **Figure 2**. Due to the presence of a 16° tilt for side profile

DOI: 10.1002/smll.201200470

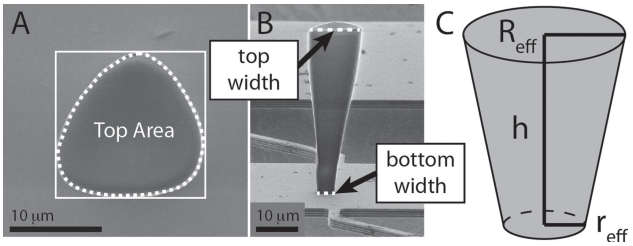

Figure 2. Source of measures for calculating gel volume. A,B) SEM images of the top and side views of a PEGDA-DMPA hydrogel structure for calculating gel volume and mass. C) Schematic of an inverted frustum and the dimensions required for calculating the volume of the hydrogel structure to estimate the mass of the hydrogel independent of the LDV-based mass measurements.

images, h is the corrected h' using a cosine function ($h = h'\cos 16°$). The equation for the frustum volume calculation is $V = \frac{1}{3}\pi\left(r_{\text{eff}}^2 + r_{\text{eff}} R_{\text{eff}} + R_{\text{eff}}^2\right) h$, where R_{eff} is the effective top radius and is obtained using $R_{\text{eff}} = \sqrt{(A/\pi)}$ assuming the area of a circle, and r_{eff} is the effective bottom radius and is obtained using $r_{\text{eff}} = R_{\text{eff}}/(w_{\text{top}}/w_{\text{bottom}})$. Because these dimensions are from SEM images of dry gel structures, the volume calculations are adjusted to account for swelling of the mass of the hydrated structures (see Experimental Section for hydrogel swelling). To obtain the estimated PEGDA hydrogel mass, the calculated volumes (V_{h}) are multiplied by the hydrogel density (ρ) of 1.124 g/cm^3.

2.7. Measuring Hydrogel Swelling

To calculate the hydrated mass of hydrogel microstructures from SEM images, the swelling of 100% PEGDA-DMPA hydrogels was characterized to produce a swelling offset. Swelling of PEGDA-DMPA microstructures is measured differently from bulk discs. The swelling offset is obtained for each microstructure; the diameter of each hydrated gel structure measured with confocal microscopy is divided by the diameter of the same air-dried structure (obtained from the SEM images). The swelling offsets are imposed on the dry volume data to give the hydrated volume (V_{h}) estimate. Confocal microscopy reveals the hydrated structures being between 1.14- and 1.26-fold greater (average = 1.19) than the same dried structure imaged in the SEM. The measured swelling offset is used for estimating the mass of PEGDA-DMPA microstructures.

To measure swelling of bulk PEGDA-DMPA hydrogel structures independent of the MEMS measurements and photolithography of gel microstructures, bulk hydrogel discs are fabricated by dispensing pre-polymer (200 μL) into the detached cap of a microcentrifuge tube (1.5 mL). The bulk PEGDA-DMPA hydrogel discs are photopolymerized with 365 nm UV light, removed from the molding structure, weighed, and immediately immersed in DI water to achieve equilibrium (24–30 h) prior to processing.

Two separate methods are used in this work to describe changes to the hydrogels as a result of hydration and dehydration. First, the degree of swelling (Q-factor) calculations are performed by factoring the densities of the polymer and water, and the calculated mass swelling ratio. The mass swelling ratio Q_m is measured from the initial and final gel mass of hydrated and completely dehydrated structures, for microstructures the hydrated and dehydrated masses were measured with the MEMS sensors.[3] Lastly, the volume of the swollen gel (V_{s}) is estimated using $V_{\text{s}} = (v_{\text{i}}(d_{\text{s}}/\, d_{\text{i}})) - v_{\text{i}}$ where v_{i} is the initial gel volume (200 μL), d_{s} is the diameter of the swollen hydrated gel, and d_{i} is the diameter of the initial gel. The PEGDA-DMPA hydrogel bulk disc diameters are measured immediately after photopolymerization and again after hydration using microscopy and a quartz micrometer.

3. Results and Discussion

Figure 1A shows the PEGDA-DMPA polymer fabrication process, a diagram of the measurement system, and a SEM image of a hydrogel microstructure fabricated on the MEMS resonant mass sensor. **Table 1** shows raw data of photolithographically defined microstructures; the data is representative of the microstructure size range.

MEMS resonant mass sensor arrays are fabricated and calibrated for the mass sensing procedure by in-air and in-liquid resonant frequency measurements,[10] prior to fabricating the hydrogel structures. In order to measure the mass of the hydrogels, a PDMS fluidic chamber is assembled on the chip to keep the gel and sensors hydrated (Figure 1A) during measurements. Laser Doppler vibometry (LDV) is used to measure the resonant frequency of the sensor with gel (Figure 1B), and the images of the sensor and hydrogel were captured for visual verification. Figure 1C shows an electron micrograph of a hydrogel frustum fabricated on the MEMS sensor using photolithography.

Table 1. Raw data representative of photolithographically defined 100% PEGDA-DMPA microstructures and the corresponding estimated frustum volumes.

Top Area [μm^2]	Effective Top Radius [μm] = R_{eff}	Effective Bottom Radius [μm] = r_{eff}	Adjusted Height [μm]	Aspect Ratio	Average Swelling Offset	Estimated Frustum Volume [cm^3] = V
485.8	12.4	6.9	50.5	2.5	1.19	1.52×10^{-8}
600.2	13.8	8.5	53.8	2.3	1.19	2.15×10^{-8}
150.6	6.9	2.4	45.9	4.8	1.19	3.40×10^{-8}
388.4	11.1	4.6	56.9	3.5	1.19	1.17×10^{-8}
298.2	9.7	3.4	55.1	4.1	1.19	8.05×10^{-9}

small 2012,
DOI: 10.1002/smll.201200470

NANO MICRO small

By calculating the mass using volume and density measurements,[10] we can compare the relationship between the measured mass obtained from the sensor and the theoretical mass; this allows us to determine potential effects of measuring tall structures and structures with a high center of mass. For example, in our previous work on measuring cell mass and growth of adherent cells, "missing mass events" occurred as cells balled up and partially detached from the sensor surface during mitosis.[10]

As shown in Figure 2, inverted conical frustums have a high center of mass and low surface area of attachment relative to the mass distribution throughout the microstructure. Volume calculations of hydrogel structures used dimensions obtained from SEM images. Dimensions for the area (A) of the hydrogel top, the gel height (h'), the top width (w_{top}), and the gel bottom width (w_{bottom}) were used to calculate the volume of a frustum for estimating structure volume (Figure 2). Because these dimensions are from SEM images of dry gel structures, the volume calculations are adjusted to account for swelling of the mass of the hydrated structures (see Section 2 for hydrogel swelling). To obtain the estimated PEGDA-DMPA hydrogel mass, the calculated volumes (V_h) are multiplied by the hydrogel density (ρ) of 1.124 g/cm^3.

Figure 3 shows the results of measured and calculated mass values for hydrogel microstructures. Here, we demonstrate that micrometer-scale hydrogel substrates can be integrated with MEMS resonant mass sensors for resolving mass and swelling of stiff (1.6–1.8 MPa)[16] PEGDA-DMPA hydrogel structures using our MEMS resonant mass sensors. Figure 3A shows the range of mass values of hydrated gels measured in water with the LDV system for each sensor number on the chip, and Figure 3B shows 4 gel structures on sensors for the corresponding measured and theoretical mass data shown in Figure 3C.

Our results show that the relationship between measured and estimated masses are linear, with an average slope of 1.07 and a good data fit ($R^2 = 0.97$). Deviations of data points from the linear trend line can be explained by small imperfections (e.g., sidewalls visible in Figure 2B) in fabricated structures which contribute to small differences in the volume-mass estimate. Previous models show that as the Young's modulus and viscosity of a sample increases to >100 kPa, the measured mass of the sample on the resonant mass sensor is equal to the actual mass of the sample.[10] Here, our results are in agreement with that model.

Volume changes are important material considerations for determining swelling and can influence mass readings for gels in our system. For example, to produce the estimated mass of hydrated PEGDA-DMPA structures, we used confocal microscopy of the hydrated gels structures and SEM images of the same gel to apply a swelling offset to the dry dimensions.

Material swelling is a key factor to consider when working with hydrogel constructs. A common term used to quantitatively describe the swelling of hydrogel materials is the "mass swelling ratio" or the Q_m.[3,17] Q_m is an accurate measure of the maximum change in water content between hydrated and dehydrated gels, because Q_m is a ratio of the hydrated and dry mass values. The Q-factor is another mass-dependent measure of the degree of swelling that takes into account the density of the polymer and hydrating solution; the Q-factor equation (Equation 1) incorporates Q_m and accounts for the material and fluid densities but it does not report a change in volume for the gel. Thus, both Q_m and the Q-factor are mass-dependent measures and do not report a change in volume.

$$Q = v_2^{-1} = \rho_P \left(\frac{Q_m}{\rho_S} + \frac{1}{\rho_P} \right) \quad (1)$$

For comparison, we determined the degree of swelling (Q-factor) in water for both the 100% PEGDA-DMPA microstructures and bulk discs using our sensors and conventional methods, respectively. **Figure 4**A shows the Q-factor of bulk structures for a range of concentrations; the data shows a strong agreement between the Q-factor of 100% PEGDA-DMPA bulk discs and microstructures (Figure 4A, inset). These results demonstrate that our MEMS mass sensors are suitable tools for measuring gel mass and

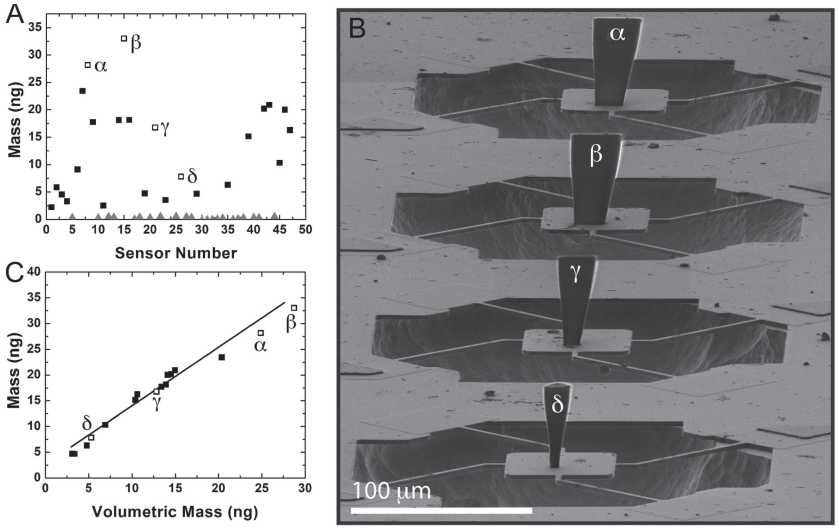

Figure 3. Measured and calculated mass of 100% PEGDA-DMPA microstructures. A) Mass values obtained from 46 sensors for hydrogel structures (squares) and empty sensors (gray triangles). Each data point represents an individual structure or empty sensor. B) SEM image of 4 sensors with PEGDA-DMPA microstructures fabricated on the sensor surface through photolithography, corresponding mass values for these structures is shown in the accompanying graphs. C) "Mass (ng)" values obtained from MEMS sensors for PEGDA-DMPA hydrogels are plotted against the "Volumetric Mass (ng)" of the same structures. The volumetric mass of the same structure is independently derived by measuring the structure volume from SEM images and multiplying the volume by density (mass = density ∗ volume). Slope of the solid line for all data points is 1.07 with an R^2 of 0.97, showing a high degree of agreement between calculated and measured masses. A–C) Open squares marked with Greek letters are for corresponding data points, demonstrating mass values for a range of hydrogel sizes.

DOI: 10.1002/smll.201200470

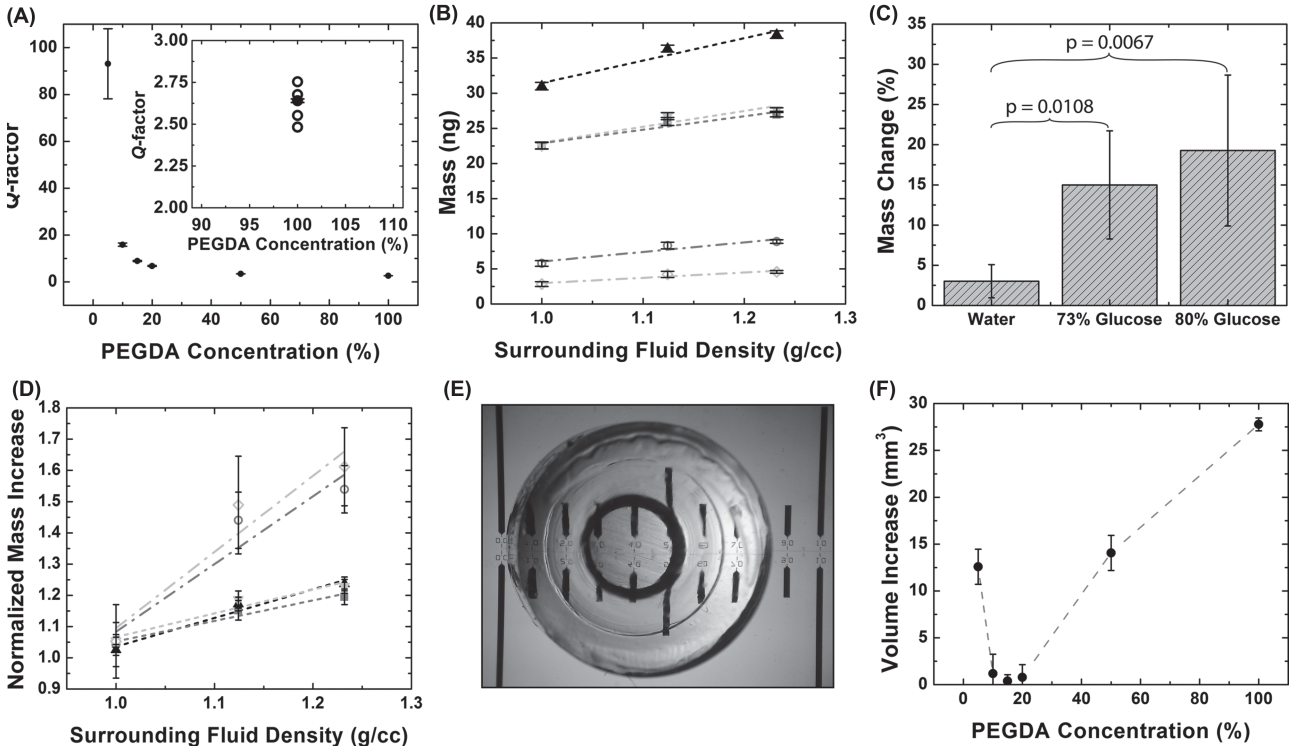

Figure 4. Swelling and mass changes of PEGDA-DMPA hydrogels. A) The *Q*-factor (a mass-based measure for degree of swelling) calculated for a range of PEGDA-DMPA concentrations, the data is based on the initial hydrated and final dehydrated mass values for bulk discs (solid black circles). Inset: Comparison of *Q*-factor measures for 100% PEGDA-DMPA hydrogels from bulk discs (black circle, $n = 3$, mean ± SD) and for microstructures fabricated with photolithography (open circles, 5 individual gels). Mass of hydrated and dried microstructures was measured using MEMS resonant sensors. B) The MEMS-measured mass values for 100% PEGDA-DMPA hydrogel structures, covering a range of structure sizes, show corresponding increases with increasing density of the surrounding fluid. Feature sizes in the range shown in Figure 3, three separate measures each point,mean ± SD. C) The percent change of apparent mass values of data for 100% PEGDA-DMPA gels (B) in higher density fluids is statistically significant from the initial and final mass measurement in water (mean ± SD, unpaired *t*-test). Fluid density is 0.99 g/cm^3 for water (24 °C), 1.13 g/cm^3 for 73% glucose in DI water, and 1.23 g/cm^3 for 80% glucose in DI water. The mass change for water is a comparison of the initial and final measurement in water before and after changing the fluid density for 73% and 80% glucose. D) Normalized apparent mass for the 100% PEGDA-DMPA hydrogel data of (B) shows that smaller structures (data sets with open shape and dash-dot trendlines) show a greater normalized mass change than larger structures (data sets with solid shapes and dashed trendlines). The data sets are normalized values from the same sample structures for graph B, three separate measures each point,mean ± SD. E) Image of a bulk hydrogel disc used to calculate the *Q*-factor in (A) and the volume change of swelling in (F). F) Volume increase of bulk hydrogel discs for a range of PEGDA-DMPA concentrations after 30 h of water incubation, $n = 3$, mean ± SD. Hydration produces substantial increases in gel volume from pre-hydration volume (200 mm^3 for all bulk gels) for 5%, 50% and 100% gels. Average hydrated volumes are 212.5 mm^3 for 5% gels, 214.0 mm^3 for 50% gels, and 227.8 mm^3 for 100% gels.

determining mass swelling ratios for materials characterization of microstructures. In addition, the data presented here for stiff structures is in agreement with the previously published analytical model for mass measurement of viscoelastic materials.[10]

Our previous cellular data and our current hydrogel data are at the ends of a wide range of material stiffness values (4.1 to 1600+ kPa), thus to more accurately validate models of viscoelastic materials in the mass-spring-damper system, data sets distributed throughout the range of stiffness values will be the focus of future investigations. These datasets should include a variety of polymer concentrations to achieve a range of material stiffness values. Photolithography of lower percent, highly aqueous, hydrogel pre-polymers produces poorly defined, amorphous gels (data not shown) due to the complexities of internal light reflection and refraction inherent with photolithography. Therefore, the deposition of soft, highly aqueous hydrogels on our sensors will need to be achieved through other means; for example, electrohydrodynamic jetting.

With the ability to accurately measure the mass of stiff hydrogels and perform mass characterization measures (Q_m and *Q*-factor) with our sensor arrays, we measured the change in mass for PEGDA-DMPA hydrogels in aqueous solutions of increased fluid density to determine how the differences between the gel and immersion media densities influence the measured mass. The results for hydrogels attached to MEMS resonant sensors show an increase in apparent mass for an increased fluid density of the surrounding solution. Figure 4B shows a density-dependent increase in hydrogel mass values for 5 separate gel structures as measured in the following sequence of aqueous fluids with respective densities; water (0.99 g/cm^3), 73% glucose in water (1.13 g/cm^3), and 80% glucose in water (1.23 g/cm^3). **Table 2** shows the corresponding resonant frequencies for 73% glucose; 1.13 g/cm^3 is a density-matched solution similar to that of the hydrogel

DOI: 10.1002/smll.201200470

NANO MICRO small

Table 2. Raw frequency data from LDV measurements of 100% PEGDA-DMPA microstructures provides mass values for Figure 4B–D. Microstructures are within the mass and size range shown in Figure 3.

Dry Frequency in Air [kHz]	Wet Frequency Empty [kHz]			Wet Frequency with Gel [kHz]		
	DI water	73% Glucose	80% Glucose	DI water	73% Glucose	80% Glucose
162.197	64.354	54.068	52.663	58.910	50.289	48.936
142.585	56.045	46.479	45.193	54.949	45.730	44.361
138.829	54.795	45.439	44.129	48.511	41.189	39.972
140.531	55.391	45.834	44.549	50.568	42.802	41.602
140.764	55.518	45.918	44.687	55.202	45.969	44.633

(1.124 g/cm^3). Figure 4C shows a statistically significant change in the apparent mass values for gels measured in matched and higher density solutions when compared to the initial measurement of the hydrogels in water. For comparison, the average differences between the final water-based hydrogel measurements to the initial water-based measurement are also shown as "water."

Given the density-dependent increase in swelling for 100% gels, the mass increase data from Figure 4B is normalized and plotted in Figure 4D to determine if an increase in the hydrodynamic loading is responsible for the mass increase. We expect that the hydrodynamic loading of the increasing density and viscosity of the surrounding fluid plays a role in the fluid density-dependent change in mass values, but how much of an effect has yet to be resolved completely.[18]

Figure 4D shows the normalized gel mass across the range of fluid densities; the shape and gray-scale-coded data labels enable a comparison of mass increase according to gel size in the corresponding Figure 4B. With larger structures there is a smaller relative change in mass from the initial structure for increasing solution densities, whereas the smaller structures are more affected by the change in fluid density. This result is in contrast to expected effects if hydrodynamic loading is the dominant influence for the mass change.

The total mass of the sensor with the gel is the sum of the gel mass, sensor mass and hydrodynamic loading of the fluid. The hydrodynamic loading increases with higher fluid density and viscosity. In addition, as the gel increases in volume, the gel-on-sensor structure has an increased surface area, which will influence the platform-sample acceleration and directly increase the induced mass. Thus, larger structures would have a greater induced mass over smaller structures if hydrodynamic loading was the dominant contributor to the size-dependent change. This suggests that the difference in gel mass attributed to the increasing solution density is not entirely due to hydrodynamic loading, but that some other factor influences these results.

Gels are water permeable and known to swell upon hydration, thus two other possible contributions include disproportionate changes in volume or density. For the former, a change in volume occurs during structure swelling, the completeness of swelling may influence the size-dependent change in mass reading. The *Q*-factor data suggest a small change in the swelling of 100% PEGDA-DMPA gels, but this measure does not report a change in structure size. To better determine how swelling changes the structure size of 100% PEGDA-DMPA microstructures, we measured the volume change of bulk PEGDA-DMPA discs between pre- and post-hydration states. Figure 4E is a representative image of the bulk discs used to determine the *Q*-factor of a range of gel formulations in Figure 4A and the volume increase for swelling of 100% PEGDA-DMPA gels shown in Figure 4F.

Figure 4F shows the change of hydrogel volume for bulk hydrogel discs that occurs between photopolymerization and 30 h of hydration in DI water; results are averages of three separate hydrogel discs for each data point for a total of 18 discs. As a result, higher gel concentrations (50% and 100%) show greater swelling compared to lower percent gels, with the exception of the 5% gel. It is clearly evident from volume swelling measures that stiff 100% PEGDA-DMPA structures exhibit the greatest volume increase compared to softer gels of decreased PEGDA-DMPA composition (Figure 4F). The change in gel volume for bulk hydrogel discs provides an added perspective to the mass-based *Q*-factor. This large amount of swelling could be explained by the increased osmotic pressures of high percent gels. Although the 100% PEGDA-DMPA gel has a greater stiffness than lower percent PEGDA-DMPA gel compositions, the material stiffness does not override the polymers capacity to swell. Data for the 5% gels suggest that the polymer network is weak enough to give way to the osmotic pressure to yield a robust change in the gel dimensions, and the 15% gel appears to be balanced by the osmotic pressure and the polymer stiffness (Figure 4F).

A size-dependent change in microstructure density could possibly explain the size-dependent mass change in fluids of increasing density. A change in the microstructure density is the combination of a number of influences. 1) Surface-area-to-volume ratio: Smaller structures have a greater surface-area-to-volume ratio than larger structures. From Fick's first law of diffusion, the diffusion flux, the amount of substance that flows per unit area per unit time, would increase with the smaller structure, because of the larger glucose concentration gradient between the inner gel and bulk media. Basically, J is related to dC/dx, where dC is the concentration change and dx is the distance of diffusion. The smaller sample should have the larger dC/dx. 2) Polymer pore size: As the polymer swells the polymer pore size changes, pore size and distribution will influence the rate of diffusion throughout the polymer structure and the time required for the gel to reach equilibrium with the surrounding fluid. If gel swelling is

DOI: 10.1002/smll.201200470

neither uniform nor complete, then larger structures may not have uniform pore sizes or glucose distribution compared to smaller structures, alternatively the structure may take longer to achieve equilibrium.

Taken together, it is possible that smaller PEGDA-DMPA gel microstructures could achieve a greater density and mass of the more dense media (i.e., increased glucose) through diffusion by achieving equilibrium with the surrounding fluid prior to their larger counterparts. To further answer this outstanding question and validate these possibilities, hydrogel microstructures of various compositions should be measured to observe the size-dependent change for gels that show different percent swelling increases according to the range of gel compositions.

4. Conclusion

We conclude that micrometer-scale hydrogel structures can be affixed to MEMS resonant sensors to measure the gel mass for materials characterization. Our results show a quantitative method for measuring mass and swelling of hydrogel microstructures, from which we conclude that gel size and stiffness influence the swelling and diffusion of substances into the gel. Furthermore, increased mass values obtained by elevating fluid densities of immersion media are observed, our data suggests that a confluence of multiple factors contribute to this observation. Future work will focus on resolving these complexities and on characterizing hydrogels of different viscoelastic properties to validate and expand models of mass-spring-damper systems for measuring soft materials and biological samples with resonant sensors. Due to the high refractivity of aqueous solutions, methods other than photolithography (e.g., electrohydrodynamic jetting) must be implemented for depositing hydrogels of all gel compositions (5%–100%) onto the platform sensor to answer these questions.

Acknowledgements

The authors would like to acknowledge and express gratitude to Vincent Chan, Brian Dorvel, Mitch Collens and Max Rich for their respective assistance with hydrogel protocols, surface chemistry, equipment training, and for providing insightful discussions; to Scott Robinson at the Beckman Institute ITG facility at the University of Illinois at Urbana-Champaign for assistance in SEM setup for quantitative measures of gel structures; and to Katrina Keller for her support in preparing sensor arrays. Funding was for this study was provided by NSF STC, Emergent Behavior in Integrated Cellular Systems CBET-0939511. E.A.C. was funded at UIUC from NSF Grant 0965918 IGERT: Cellular and Molecular Mechanics and BioNanotechnology.

[1] a) J. J. Schmidt, J. Jeong, H. Kong, *Tissue Eng. A* **2011**, *17*, 2687–2694; b) Y. Liang, J. Jeong, R. J. DeVolder, C. Cha, F. Wang, Y. W. Tong, H. Kong, *Biomaterials* **2011**, *32*, 9308–9315.
[2] a) T. R. Hoare, D. S. Kohane, *Polymer* **2008**, *49*, 1993–2007; b) Y. M. Kolambkar, K. M. Dupont, J. D. Boerckel, N. Huebsch, D. J. Mooney, D. W. Hutmacher, R. E. Guldberg, *Biomaterials* **2011**, *32*, 65–74; c) X. Zhao, J. Kim, C. A. Cezar, N. Huebsch, K. Lee, K. Bouhadir, D. J. Mooney, *Proc. Natl. Acad. Sci. USA* **2011**, *108*, 67–72.
[3] V. Chan, P. Zorlutuna, J. H. Jeong, H. Kong, R. Bashir, *Lab Chip* **2010**, *10*, 2062–2070.
[4] P. Tayalia, E. Mazur, D. J. Mooney, *Biomaterials* **2011**, *32*, 2634–2641.
[5] G. D. Nicodemus, S. J. Bryant, *Tissue Eng. B* **2008**, *14*, 149–165.
[6] V. Chan, J. H. Jeong, P. Bajaj, M. Collens, T. Saif, H. Kong, R. Bashir, *Lab Chip* **2012**, *12*, 88–98.
[7] a) A. Gupta, D. Akin, R. Bashir, *Appl. Phys. Lett.* **2004**, *84*, 1976–1978; b) A. Gupta, D. Akin, R. Bashir, 18th Int. Conf. Micro Electro Mechanical Systems (MEMS), **2005**,
[8] a) A. Gupta, D. Akin, R. Bashir, *Proc. SPIE-Int. Soc. Opt. Eng* **2003**, *4982*, 21–27; b) A. Gupta, D. Akin, R. Bashir, *J. Vac. Sci. Tech. B.* **2004**, *22*, 2785–2791.
[9] a) K. Park, J. Jang, D. Irimia, J. Sturgis, J. Lee, J. P. Robinson, M. Toner, R. Bashir, *Lab Chip* **2008**, *8*, 1034–1041; b) A. K. Bryan, A. Goranov, A. Amon, S. R. Manalis, *Proc. Natl. Acad. Sci. USA* **2010**, *107*, 999–1004; c) M. Godin, F. F. Delgado, S. Son, W. H. Grover, A. K. Bryan, A. Tzur, P. Jorgensen, K. Payer, A. D. Grossman, M. W. Kirschner, S. R. Manalis, *Nat Methods* **2010**, *7*, 387–390.
[10] K. Park, L. J. Millet, N. Kim, H. Li, X. Jin, G. Popescu, N. R. Aluru, K. J. Hsia, R. Bashir, *Proc. Natl. Acad. Sci. USA* **2010**, *107*, 20691–20696.
[11] T. P. Burg, M. Godin, S. M. Knudsen, W. Shen, G. Carlson, J. S. Foster, K. Babcock, S. R. Manalis, *Nature* **2007**, *446*, 1066–1069.
[12] N. V. Lavrik, M. J. Sepaniak, P. G. Datskos, *Rev. Sci. Instrum.* **2004**, *75*, 2229–2253.
[13] J. N. Israelachvili, *Intermolecular and Surface Forces*, 3rd ed., Academic Press, Burlington, MA, **1992**.
[14] S. Dohn, R. Sandberg, W. Svendsen, A. Boisen, *Appl. Phys. Lett.* **2005**, *86*, 233501.
[15] K. Park, R. Bashir, Transducers, Denver, CO **2009**.
[16] Z. Drira, *PhD Thesis*, Virginia Commonwealth University, Richmond, VA, **2009**.
[17] a) J. A. Beamish, J. Zhu, K. Kottke-Marchant, R. E. Marchant, *J. Biomed. Mater. Res. A* **2010**, *92*, 441–450; b) S. J. Bryant, K. L. Durand, K. S. Anseth, *J. Biomed. Mater. Res. A* **2003**, *67*, 1430–1436; c) J. L. Young, A. J. Engler, *Biomaterials* **2011**, *32*, 1002–1009.
[18] S. Basak, A. Raman, S. V. Garimella, *J. Appl. Phys.* **2006**, *99*.

Received: March 1, 2012
Revised: April 11, 2012
Published online:

DOI: 10.1002/smll.201200470